AIP | APL Materials

Structural and electronic properties of hybrid perovskites for high-efficiency thin-film photovoltaics from first-principles

Federico Brivio, Alison B. Walker, and Aron Walsh

Citation: APL Materials **1**, 042111 (2013); doi: 10.1063/1.4824147
View online: http://dx.doi.org/10.1063/1.4824147
View Table of Contents: http://scitation.aip.org/content/aip/journal/aplmater/1/4?ver=pdfcov
Published by the AIP Publishing

APL MATERIALS **1**, 042111 (2013)

Structural and electronic properties of hybrid perovskites for high-efficiency thin-film photovoltaics from first-principles

Federico Brivio,[1] Alison B. Walker,[2] and Aron Walsh[1,a]
[1]*Centre for Sustainable Chemical Technologies and Department of Chemistry, University of Bath, Claverton Down, Bath BA2 7AY, United Kingdom*
[2]*Department of Physics, University of Bath, Claverton Down, Bath BA2 7AY, United Kingdom*

(Received 14 August 2013; accepted 20 September 2013; published online 10 October 2013)

The performance of perovskite solar cells recently exceeded 15% solar-to-electricity conversion efficiency for small-area devices. The fundamental properties of the active absorber layers, hybrid organic-inorganic perovskites formed from mixing metal and organic halides [e.g., $(NH_4)PbI_3$ and $(CH_3NH_3)PbI_3$], are largely unknown. The materials are semiconductors with direct band gaps at the boundary of the first Brillouin zone. The calculated dielectric constants and band gaps show an orientation dependence, with a low barrier for rotation of the organic cations. Due to the electric dipole of the methylammonium cation, a photoferroic effect may be accessible, which could enhance carrier collection. [http://dx.doi.org/10.1063/1.4824147]

Progress in the performance of hybrid pervoskite solar cells has rapidly advanced over the last five years.[1–6] They represent the convergence of inorganic thin-film and dye-sensitised solar cells.[7] The conversion efficiencies have quickly surpassed both those of conventional dye-cells, as well as next-generation thin-film absorbers such as Cu_2ZnSnS_4.[8,9] Despite their high-performance for small area (~0.2 cm^2) cells, the underlying material properties are largely unknown, which could help with producing more robust large-area devices.

Perovskite refers to the crystal structure of the mineral $CaTiO_3$, which is adopted by a large family of ABX_3 materials, with two notable examples being $SrTiO_3$ and $BaTiO_3$ (Figure 1). They are well known for their phase complexity, with accessible cubic, tetragonal, orthorhombic, trigonal, and monoclinic polymorphs depending on the tilting and rotation of the BX_6 polyhedra in the lattice.[10] Phase transitions are frequently observed under the influence of temperature, pressure, and/or applied electric field.

While oxide perovskites (ABO_3) are formed from divalent A^{II} (1*b* site – cuboctahedral) and tetravalent B^{IV} (1*a* site – octahedral) metals, halide perovskites (e.g., ABI_3) can be formed from monovalent A^{I} and divalent B^{II} metals. For example, the application of $CsSnI_3$ in solar cells has recently been demonstrated.[11] Hybrid organic-inorganic perovskites are produced by replacing one of the inorganic cations by an isovalent molecule, e.g., $CsSnI_3 \rightarrow (NH_4)SnI_3$, where NH_4^+ (A) is the ammonium cation. Recently, the methylammonium (MA) cation (i.e., $CH_3NH_3^+$) has been widely applied, resulting in the highest-performance perovskite-structured photovoltaic absorbers.[2,3] More generally, a large series of hybrid perovskites have been reported, which vary in their dimensionality and the orientation of the underlying perovskite lattice.[12–15]

In this letter, we assess the properties of the two archetypal hybrid perovskites $(NH_4)PbI_3$ and $(CH_3NH_3)PbI_3$ using density functional theory (DFT) for the ground-state properties and density functional perturbation theory (DFPT) for the dielectric and optical response functions. We provide

[a]Electronic mail: a.walsh@bath.ac.uk

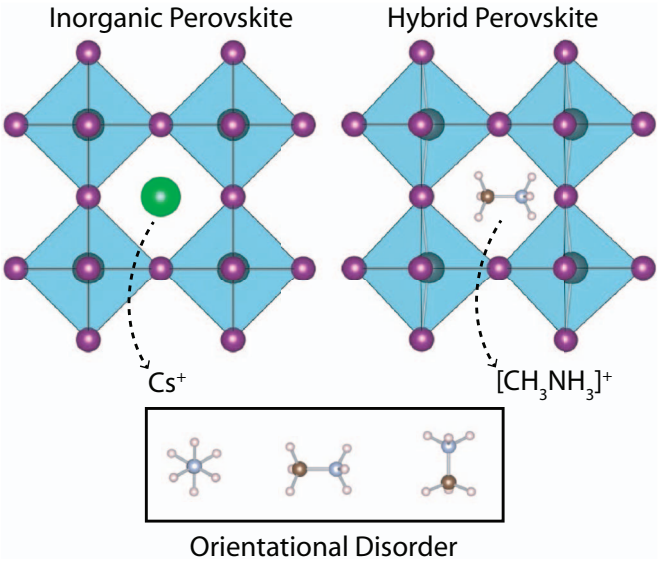

FIG. 1. Illustration of the perovskite structure based on corner sharing octahedra of BX_6 with either a monovalent metal (inorganic) or charged molecule (hybrid) at the centre of the unit cell. For hybrids, there is an orientation dependence on the central cation.

insights into the key properties required for device models and screening procedures and that underpin their utility in photovoltaic cells.

Characterisation of the crystal structures of inorganic perovskites is difficult, and hybrid perovskites are even more challenging. Recent analysis of high-quality (MA)PbI_3 crystals identified cubic ($Pm\bar{3}m$), tetragonal ($I4/mcm$), and orthorhombic ($Pnam$) phases from X-ray diffraction, while transmission electron microscopy suggested a pseudo-cubic behaviour that is consistent with variability in the octahedral titling and/or rotations.[16] For our investigation, we take a cubic basis, starting from the $Pm\bar{3}m$ lattice, and investigate the potential energy landscape associated with the molecular orientation.

The crystal structures (internal forces and external pressure) were optimised at the level of DFT, with the exchange-correlation functional of Perdew, Burke, and Ernzerhof revised for solids (PBEsol).[17] The Pb 5*d* orbitals were treated as valence and scalar-relativistic effects are included. Further calculations were made using a non-local hybrid exchange-correlation functional (HSE06).[18] Calculations were performed using the VASP code,[19] a 500 eV plane-wave cut-off, and reciprocal space sampling of $6 \times 6 \times 6$ *k*-point density. Internal structural parameters were converged to within 5 meV/Å, and the phonon frequencies were checked at the zone-centre to ensure that no imaginary modes were present. The high-frequency (ϵ_∞) and static (ϵ_0) dielectric constants were computed using DFPT[20] based upon a tightly converged electronic wavefunction (within 10^{-9} eV) and a denser grid of $10 \times 10 \times 10$ *k*-points.

For (A)PbI_3 there is no strong orientation dependence of the ammonium ion owing to its approximately spherical topology. A local minimum structure is found where the four hydrogens are directed towards interstitial positions. For (MA)PbI_3 the behaviour is more subtle owing to a molecular dipole (of strength 2D) associated with the methylammonium ion (i.e., $[CH_3]^{\delta+} - [NH_3]^{\delta-}$). We identified three local minima, where the dipole is aligned along of the ⟨100⟩, ⟨110⟩, and ⟨111⟩ directions, relative to the origin of the cubic lattice (Figure 1). The total energy difference is within 15 meV per atom, with the ⟨100⟩ orientation being most stable. The absence of a significant barrier to rotation (<40 meV) is consistent with labile movement under standard conditions. Indeed, ^{2}H and ^{14}N spectra have confirmed that MA cation rotation is a rapid process at room temperature.[21]

The predicted lattice constants for (MA)PbI_3 vary from 6.26 to 6.29 Å (Table I) depending on the molecular orientation. These compare well to the value of 6.26 Å obtained from powder diffraction measurements[16] and 6.33 Å from computations.[22] Distortions of the PbI_6 octahedra are observed for

TABLE I. Predicted materials properties of hybrid perovskites, from density functional theory (PBEsol functional), where (MA) refers to the CH_3NH_3 cation. The diagonal of the dielectric tensors is given as ϵ^{xx}, ϵ^{yy}, and ϵ^{zz}.

Material	a (Å)	E_g (eV)	ϵ_0	ϵ_∞
$(NH_4)PbI_3$	6.21	1.20	18.62, 18.47, 18.14	6.49, 6.49, 6.47
$(MA)PbI_3$ – ⟨100⟩	6.29	1.38	22.39, 27.65, 17.97	6.29, 5.89, 5.75
$(MA)PbI_3$ – ⟨110⟩	6.26	1.37	17.95, 23.56, 22.67	5.62, 6.54, 6.26
$(MA)PbI_3$ – ⟨111⟩	6.28	1.37	36.52, 37.28, 24.94	6.10, 6.10, 5.92

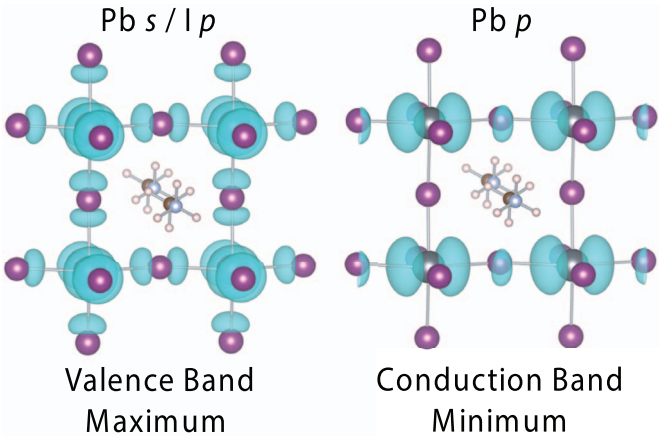

FIG. 2. Isosurface plot of the self-consistent electron density associated with the PBEsol Kohn-Sham wavefunctions of the upper valence and lower conduction bands of $(MA)PbI_3$.

both materials, even within the cubic basis. The presence of the molecule lowers the internal lattice symmetry of the parent perovskite structure and allows octahedral tilting to take place. The inherent structural "softness" of Pb(II) is well documented, arising from the stereochemical activity of the $6s^2$ lone pair electrons.[23]

The electronic band gap is determined by the states at the valence band maximum (VBM) and conduction band minimum (CBM). For both materials, the VBM is formed of an anti-bonding Pb *s*/I *p* combination, while the CBM is formed of empty Pb *p* orbitals, consistent with the formal electronic configuration of $5d^{10}6s^26p^0$. From the topology of the band-edge wave functions (Figure 2) isotropic hole and electron band conduction is expected. The strong dispersion of the bands in reciprocal space, confirmed from E(k) plots with m_n^* and $m_p^* < 0.3\ m_e$, is consistent with the reports of effective bipolar electrical conductivity.[24] A dedicated study of the defect physics is required to fully assess the origin of intrinsic conductivity, but partial occupancy of the organic cation sites is likely, which would correspond to *p*-type doping.

The magnitude of the band gap determines the onset of optical absorption and is closely related to the maximum voltage achievable in a photovoltaic device. The gap increases from 1.20 eV for $(A)PbI_3$ to 1.38 eV for $(MA)PbI_3$ (Table I). In all cases, the band gap is strongly direct and determined at the boundary of the first Brillouin zone ($R : \frac{2\pi}{a}[\frac{1}{2}, \frac{1}{2}, \frac{1}{2}]$). The increase is related to the significant expansion of the cell due to the larger cation: there is no evidence of M or MA contributing electronically to the frontier orbitals. In agreement with our results, a previous investigation of Sn-based hybrids showed that while the organic cations maintain overall charge neutrality, implying electronic mixing with the framework, they do not contribute the upper valence or lower conduction band states responsible for conductivity.[15] Indeed, the σ/σ^* bonds of A and MA are found at least 5 eV below the highest occupied state and 2.5 eV above the lowest empty state, respectively.

Although the application of hybrid perovskites in solar cells has predominately focused on $(MA)PbI_3$, our results suggest that $(A)PbI_3$ would also be effective for sensitisation towards longer wavelengths, and an $(A)_x(MA)_{1-x}PbI_3$ alloy could be used to tune the absorption onset. It should be

noted that the same trends calculated with PBEsol are observed using the hybrid HSE06 functional; however, the predicted band gaps are larger. Optical absorption measurements place the band gap of (MA)PbI_3 at 1.5 eV,[16] while PBEsol and HSE06 predict values close to 1.4 eV and 2.0 eV, respectively. The calculated band gaps for materials formed by ns^2 cations such as Pb(II) are reasonably described without non-local electron exchange.[25,26] This originates here from a cancellation of errors with the neglect of spin-orbit splitting in the I 5*p* valence and Pb 6*p* conduction bands.[27]

Due to the pseudo-cubic lattice symmetry, the dielectric response of the hybrid materials is anisotropic (Table I). The high-frequency optical constants (5.6–6.5) are close to those of other absorber materials, e.g., $\epsilon_{\infty}^{CdTe} = 7.1$;[28] however, the static dielectric response is much larger. The large dielectric constants of pervoskite materials are associated with the structural flexibility that can support ferro-, anti-, and para-electric ordering of dipoles associated with the organic and/or inorganic sublattices. (A)PbI_3 is predicted to have low-frequency constants from 18.1 to 18.6, while (MA)PbI_3 exhibits a stronger screening of 18.0–37.3, which can be understood through the additional response from the molecular dipole in (MA)PbI_3. An isotropic average of the tensor across each orientation results in an effective dielectric constant of 25.7 for (MA)PbI_3, which is significantly larger than most tetrahedral semiconductors (e.g., $\epsilon_0^{CdTe} = 10.4$)[28] and will affect electron transport in a photovoltaic device, with stronger screening of any macroscopic electric fields across the absorber layer.

An order-disorder transition associated with the molecular dipole of MA, in a perovskite analogue, has recently been reported to give rise to reversible switching in the dielectric response.[29] While no evidence has been reported of this effect in hybrid halide perovskites, it is expected that they will also display some degree of amphidynamic behaviour arising from the collective motion of the constituent polar molecules. Tuning of the molecular dipoles represents a potential route for further improving the performance of this class of materials.

In summary, we have reported key properties of the hybrid perovskite layers used in thin-film solar cells. These materials combine low-energy direct band gaps with static dielectric constants larger than 18. Due to the low barrier for rotation of the organic cations, no long-range ordering of the molecular dipoles associated with CH_3NH_3 is expected; however, this could change in the presence of an external electric field. A transition from para- to ferroelectric order would enhance electron-hole separation. If the electric field was light induced, e.g., in a photovoltaic device, this could give rise to a novel photoferroic effect.

We thank L. M. Peter, K. T. Butler, and P. J. Cameron for useful discussions, and acknowledge membership of the UK's HPC Materials Chemistry Consortium, which is funded by EPSRC Grant No. EP/F067496. F.B. is funded through the EU DESTINY Network (Grant No. 316494). A.B.W. has received funding from EPSRC Grant No. EP/J017361/1, and A.W. acknowledges support from the Royal Society and the ERC (Grant No. 277757).

[1] A. Kojima, K. Teshima, Y. Shirai, and T. Miyasaka, J. Am. Chem. Soc. **131**, 6050 (2009).
[2] M. M. Lee, J. Teuscher, T. Miyasaka, T. N. Murakami, and H. J. Snaith, Science **338**, 643 (2012).
[3] J. Burschka, N. Pellet, S.-J. Moon, R. Humphry-Baker, P. Gao, M. K. Nazeeruddin, and M. Grätzel, Nature (London) **499**, 316 (2013).
[4] H.-S. Kim, C.-R. Lee, J.-H. Im, K.-B. Lee, T. Moehl, A. Marchioro, S.-J. Moon, R. Humphry-Baker, J.-H. Yum, J. E. Moser *et al.*, Sci. Rep. **2**, 591 (2012).
[5] J. H. Heo, S. H. Im, J. H. Noh, T. N. Mandal, C.-S. Lim, J. A. Chang, Y. H. Lee, H.-J. Kim, A. Sarkar, M. K. Nazeeruddin *et al.*, Nat. Photonics **7**, 486 (2013).
[6] M. J. Carnie, C. Charbonnaeu, M. L. Davies, J. Troughton, T. M. Watson, K. Wojciechowski, H. Snaith, and D. A. Worsley, Chem. Commun. **49**, 7893 (2013).
[7] N.-G. Park, J. Phys. Chem. Lett. **4**, 2423 (2013).
[8] T. K. Todorov, K. B. Reuter, and D. B. Mitzi, Adv. Mater. **22**, E156 (2010).
[9] A. Walsh, S. Chen, S.-H. Wei, and X.-G. Gong, Adv. Energy Mater. **2**, 400 (2012).
[10] A. M. Glazer, Acta. Cryst. **B28**, 3384 (1972).
[11] I. Chung, B. Lee, J. He, R. P. Chang, and M. G. Kanatzidis, Nature (London) **485**, 486 (2012).
[12] J. Calabrese, N. Jones, R. Harlow, N. Herron, D. Thorn, and Y. Wang, J. Am. Chem. Soc. **113**, 2328 (1991).
[13] D. B. Mitzi, S. Wang, C. A. Feild, C. A. Chess, and A. M. Guloy, Science **267**, 1473 (1995).
[14] K. Liang, D. B. Mitzi, and M. T. Prikas, Chem. Mater. **10**, 403 (1998).
[15] I. Borriello, G. Cantele, and D. Ninno, Phys. Rev. B **77**, 235214 (2008).

[16] T. Baikie, Y. Fang, J. M. Kadro, M. Schreyer, F. Wei, S. G. Mhaisalkar, M. Grätzel, and T. J. White, J. Mater. Chem. A **1**, 5628 (2013).
[17] J. P. Perdew, A. Ruzsinszky, G. I. Csonka, O. A. Vydrov, G. E. Scuseria, L. A. Constantin, X. Zhou, and K. Burke, Phys. Rev. Lett. **100**, 136406 (2008).
[18] A. V. Krukau, O. A. Vydrov, A. F. Izmaylov, and G. E. Scuseria, J. Chem. Phys. **125**, 224106 (2006).
[19] G. Kresse and J. Furthmüller, Phys. Rev. B **54**, 11169 (1996).
[20] S. Baroni, S. de Gironcoli, A. Dal Corso, and P. Giannozzi, Rev. Mod. Phys. **73**, 515 (2001).
[21] R. Wasylishen, O. Knop, and J. Macdonald, Solid State Commun. **56**, 581 (1985).
[22] E. Mosconi, A. Amat, M. K. Nazeeruddin, M. Grätzel, and F. De Angelis, J. Phys. Chem. C **117**, 13902 (2013).
[23] A. Walsh, D. J. Payne, R. G. Egdell, and G. W. Watson, Chem. Soc. Rev. **40**, 4455 (2011).
[24] C. C. Stoumpos, C. D. Malliakas, and M. G. Kanatzidis, Inorg. Chem. **52**, 9019 (2013).
[25] S.-H. Wei and A. Zunger, Phys. Rev. B **55**, 13605 (1997).
[26] A. Walsh, J. Phys. Chem. Lett. **1**, 1284 (2010).
[27] A more accurate treatment than PBEsol would be HSE06+SOC; however, this was not possible due to the high computational cost and the absence of DFPT for this level of theory.
[28] O. M. Madelung, *Semiconductors: Data Handbook*, 3rd ed. (Springer, Berlin, 2004).
[29] W. Zhang, H.-Y. Ye, R. Graf, H. W. Spiess, Y.-F. Yao, R.-Q. Zhu, and R.-G. Xiong, J. Am. Chem. Soc. **135**, 5230 (2013).